

Lawrence Berkeley National Laboratory

Lawrence Berkeley National Laboratory

Title

Design Optimization for an X-Ray Free Electron Laser Driven by SLAC Linac

Permalink

<https://escholarship.org/uc/item/0bd64575>

Author

Xie, Ming

Publication Date

1994-12-01

DESIGN OPTIMIZATION FOR AN X-RAY FREE ELECTRON LASER DRIVEN BY SLAC LINAC *

Ming Xie, Lawrence Berkeley Laboratory, Berkeley, CA 94720, USA

Abstract

I present a design study for an X-ray Free Electron Laser (FEL) driven by the SLAC linac. The study assumes the FEL is based on Self-Amplified Spontaneous Emission (SASE) and lasing is achieved in a single pass of a high current, high brightness electron beam through a long wiggler. Following a brief review of the fundamentals of SASE, I will provide without derivation a collection of formulas relating SASE performance to the system parameters. These formulas allow quick evaluation of FEL designs and provide powerful tools for optimization in multi-dimensional parameter space. Optimization is carried out for the SLAC FEL over all independent system parameters modeled, subjected to a number of practical constraints.

I. INTRODUCTION

An X-ray Free Electron Laser (FEL) driven by the SLAC linac, the Linac Coherent Light Source (LCLS) [1], was proposed to reach wavelengths down to a few Å with performance far exceeding other sources. At this wavelength range Self-Amplified Spontaneous Emission (SASE) [2][3][4] is the only working principle, since mirrors are not available to make an oscillator.

A SASE FEL, in its basic configuration, requires a high current, high brightness electron beam and a long wiggler. As the electron beam passes through the wiggler, the initial spontaneous radiation induces a longitudinal density modulation in the electron beam at the radiation wavelength scale, and as a result the spontaneous radiation becomes amplified in intensity and enhanced in coherence characteristics, leading to an exponential instability. As the optical power build up, electrons become trapped and rotate in the phase space bucket. Eventually the beam-wave interaction becomes nonlinear, putting the exponential power growth into saturation. For the LCLS, a power maximum can be reached with a wiggler a few tens of meters long.

Effectively a SASE FEL is a power amplifier. Its initiation, growth and saturation can be described simply by

$$P = \alpha P_n e^{z/L_g} < P_{sat} \quad (1)$$

where P_n is the effective input noise power, α is the coupling coefficient representing the fraction of the noise power P_n coupled into the dominant mode exponentially growing in z (the distance along the wiggler) with a power gain length L_g , and P_{sat} is the saturation power. The input noise power is the frequency integrated synchrotron radiation power in an FEL gain bandwidth generated in the first gain length or so [2][5]. Corresponding to the saturation power, one may define a saturation length given by

$$L_{sat} = L_g \ln \left(\frac{P_{sat}}{\alpha P_n} \right) \quad (2)$$

which is the length of the wiggler required to reach the maximum output power. The quantities L_g , L_{sat} and P_{sat} are the major performance parameters for SASE.

II. MODELS AND FORMULAS

An FEL amplifier consists of three major components: an electron beam from an accelerator; a wiggler for beam-wave interaction; and a focusing system for electron beam confinement in the wiggler. In this paper, the electron beam distribution is assumed to be of Gaussian shape in four dimensional transverse phase space and in the energy variable, but uniform in longitudinal coordinate. The assumption of uniform longitudinal distribution is justified for the LCLS even though the electron bunch is only a few hundred femtoseconds long, since the ratio of the bunch length to the radiation wavelength is so large that the so called short pulse effects are negligible from the FEL interaction. Further assuming round beam with equal emittance in both transverse planes we may characterize the electron beam by four parameters: beam energy $E = \gamma mc^2$; current I ; normalized rms emittance ε_n and rms energy spread σ_e . The wigglers are separated into two classes: planar and helical, each class is specified by two parameters: wiggler period λ_w and a dimensionless wiggler parameter: $K = 0.934 \lambda_w [\text{cm}] B_0 [\text{T}]$, where B_0 is the peak wiggler magnetic field.

The focusing system is assumed to have a transverse gradient invariant along the beam axis and characterized by a constant betafunction β . Such a system would give a constant beam envelope for the matched beam over the entire wiggler length. The focusing of this type is naturally provided in a wiggler, but may not be strong enough to have optimal FEL performance especially at short wavelength. To remedy this problem external focusing has been considered and alternating-gradient quadrupole was shown [6][7] to perform better than the constant gradient focusing. If this is true in general, the formulas provided in this paper would give conservative results.

Given electron beam and wiggler parameters, the radiation wavelength is determined by a resonance condition $\lambda = \lambda_w (1 + a_w^2) / 2\gamma_0^2$ where $a_w = K$ for helical and $a_w = K/\sqrt{2}$ for planar wiggler, γ_0 is related to the average beam energy E_0 .

To determine SASE performance given system parameters it is instructive to look first at the simplest model, the so called one-dimensional (1D) model [2][8]. The 1D model is an ideal case, which assumes the electron beam has a uniform transverse spatial distribution with zero emittance and energy spread. In this model the quantities appeared in Eq.(1) are given by

$$\alpha = 1/9, \quad P_n \approx \rho^2 c E_0 / \lambda \quad (3)$$

$$L_g = \lambda_w / 4\pi\sqrt{3}\rho, \quad P_{sat} \approx \rho P_{beam}$$

*This work was supported by the U.S. Department of Energy under contract No. DE-AC03-76SF00098.

where ρ is a dimensionless parameter known as the Pierce parameter [8] defined by

$$\rho = \left[\left(\frac{I}{I_A} \right) \left(\frac{\lambda_w A_w}{2\pi\sigma_x} \right)^2 \left(\frac{1}{2\gamma_0} \right)^3 \right]^{1/3} \quad (4)$$

where $I_A = 17.045$ kA is the Alfvén current, $A_w = a_w$ for helical wiggler and $A_w = a_w[J_0(\xi) - J_1(\xi)]$ for planar wiggler, $\xi = a_w^2/2(1 + a_w^2)$, J'_s are Bessel functions, electron rms beam size is determined by $\sigma_x = \sqrt{\beta\varepsilon}$, $\varepsilon = \varepsilon_n/\gamma_0$, and electron beam power is given by $P_{beam}[\text{TW}] = E_0[\text{GeV}]I[\text{kA}]$.

Notice the Pierce parameter is proportional to the cubic root of the current density. Here we have replaced the current density by the peak value, $I/2\pi\sigma_x^2$, for a Gaussian beam. Thus the 1D model gives the highest possible FEL gain (shortest gain length) and can be used as a reference for the cases with non-ideal electron beam. In fact it can be shown from rigorous analysis [9][10][11] that the FEL gain length can be expressed by a universal scaling function

$$\frac{L_{1d}}{L_g} = F(\eta_d, \eta_\varepsilon, \eta_\gamma) \quad (5)$$

where

$$\eta_d = \frac{L_{1d}}{L_r}, \quad \eta_\varepsilon = \left(\frac{L_{1d}}{\beta} \right) \left(\frac{4\pi\varepsilon}{\lambda} \right), \quad \eta_\gamma = 4\pi \left(\frac{L_{1d}}{\lambda_w} \right) \left(\frac{\sigma_e}{E_0} \right)$$

L_{1d} is the gain length given by the 1D model, Eq.(3), and Rayleigh range is defined by $L_r = 4\pi\sigma_x^2/\lambda$.

The universal scaling function, determined by fitting numerical solutions of the coupled Maxwell-Vlasov equations describing FEL interaction, is given by [11]

$$\frac{L_{1d}}{L_g} = \frac{1}{1 + \eta} \quad (6)$$

where

$$\begin{aligned} \eta &= a_1\eta_d^{a_2} + a_3\eta_\varepsilon^{a_4} + a_5\eta_\gamma^{a_6} \\ &+ a_7\eta_\varepsilon^{a_8}\eta_\gamma^{a_9} + a_{10}\eta_d^{a_{11}}\eta_\gamma^{a_{12}} + a_{13}\eta_d^{a_{14}}\eta_\varepsilon^{a_{15}} \\ &+ a_{16}\eta_d^{a_{17}}\eta_\varepsilon^{a_{18}}\eta_\gamma^{a_{19}} \end{aligned}$$

and the 19 fitting parameters are given below.

$a_1 = 0.45$	$a_2 = 0.57$	$a_3 = 0.55$	$a_4 = 1.6$
$a_5 = 3$	$a_6 = 2$	$a_7 = 0.35$	$a_8 = 2.9$
$a_9 = 2.4$	$a_{10} = 51$	$a_{11} = 0.95$	$a_{12} = 3$
$a_{13} = 5.4$	$a_{14} = 0.7$	$a_{15} = 1.9$	$a_{16} = 1140$
$a_{17} = 2.2$	$a_{18} = 2.9$	$a_{19} = 3.2$	

Notice the maximum of the scaling function corresponds to $L_{1d}/L_g = F(0, 0, 0) = 1$, which gives the shortest gain length in the 1D limit. Thus the scaling parameters η_d , η_ε , and η_γ measure the deviation of the beam from the ideal case. Specifically, η_d is for gain reduction due to diffraction, a spatial 3D effect, η_ε and η_γ are for gain reduction due to electron's longitudinal velocity spread caused by emittance and by energy spread, respectively. Another scaling parameter related to the wavelength detuning has been optimized thus eliminated to give Eq.(5) and (6).

The saturation power obtained empirically by fitting simulation results is given by [12]

$$P_{sat} \approx 1.6\rho \left(\frac{L_{1d}}{L_g} \right)^2 P_{beam}. \quad (7)$$

A formula for noise power is not available for non-ideal beam. So the 1D formula in Eq.(3) will be used instead, which is shown by simulation [13] to give conservative estimate of noise power for non-ideal beam.

III. EVALUATION AND OPTIMIZATION OF LCLS DESIGN

Using the formulas given in the previous section, a computer code is developed to evaluate SASE performance given wiggler class (planar or helical) and seven independent system parameters: I (kA), ε_n (mm-mrad), σ_e (MeV), λ_w (cm), K , β (m), and λ (Å). With the code any one of the seven parameters can either be fixed at a given value, varied or optimized over a given range, in any combination. The criteria for optimization is to have the shortest possible saturation length in order to minimize the size and hence the cost of the project. Optimization for the LCLS is carried out in three steps.

A. Wiggler Optimization

A contour plot of L_{sat} vs. λ_w and K is shown for planar wiggler in Fig.1, where the three beam parameters: I , ε_n , and σ_e are fixed at nominal values given in table 1 for $\lambda = 1.5$ Å, and β is optimized (varied to give the shortest L_{sat}) throughout this section. The calculations shown in Fig.1 are for a generic planar wiggler. In reality, the accessible area in the λ_w - K space is limited by practical constraints, such as wiggler design, beam energy, etc. For the hybrid wiggler of Nd-Fe-B type λ_w and K are related by the Halbach formula [14]: $K = 3.2\lambda_w[\text{cm}] \exp[-5.08g/\lambda_w + 1.54(g/\lambda_w)^2]$, where g is the full wiggler gap. There are two major practical constraints: one is on g , which limits the size of beam pipe thus should not be too small to cause wakefield problem; another constraint is on beam

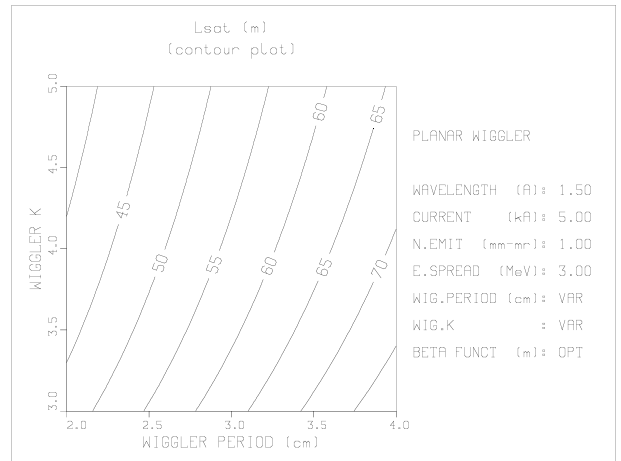


Figure 1. L_{sat} vs. λ_w and K for a generic planar wiggler.

energy, which should not exceed 15 GeV considering the availability of SLAC linac. Taking into account the two constraints, the optimized wiggler and focusing parameters: λ_w , K , and β , together with SASE performance parameters: L_g and L_{sat} are given in table 1 for three choices of g values. Also given in table 1 are the similar optimization results for a superconducting helical wiggler [15]. Beam energy is close to 15 GeV for all these cases.

Table 1. Parameters and Optimization Results

$\lambda = 1.5\text{\AA}$, $I = 5\text{kA}$, $\varepsilon_n = 1\text{mm-mr}$, $\sigma_e = 3\text{MeV}$					
Hybrid Planar Wiggler					
$g(\text{cm})$	$\lambda_w(\text{cm})$	K	$\beta(\text{m})$	$L_g(\text{m})$	$L_{sat}(\text{m})$
0.6	3.0	3.7	10	3.1	58
0.8	3.4	3.6	11	3.5	65
1.0	3.7	3.4	12	3.8	71
Superconducting Helical Wiggler					
$g(\text{cm})$	$\lambda_w(\text{cm})$	K	$\beta(\text{m})$	$L_g(\text{m})$	$L_{sat}(\text{m})$
0.6	2.0	3.4	5.1	1.4	26
0.8	2.15	3.3	5.6	1.5	28
1.0	2.3	3.1	6.1	1.7	31

B. Effects of Beam Quality

The dependence of L_{sat} on I and ε_n is shown in Fig.2 for the hybrid wiggler, with both I and ε_n varied above and below the nominal values in table 1. Notice the tradeoff possibilities between the beam quality parameters: I and ε_n suggested by the contour lines.

C. Upgrade Pass

As seen from Fig.2, operation at $\lambda = 1.5\text{\AA}$ strongly prefers high quality beam. However the requirement on beam quality is relaxed at longer wavelength. Thus one may envision an upgrade pass using the same wiggler optimized for 1.5\AA but starting at a longer wavelength with somewhat lower quality beam, and approaching 1.5\AA as beam quality improves. To illustrate this point in a single plot, let's consider a three-dimensional beam parameter space $\{I, \varepsilon_n, \sigma_e\}$. Suppose the operation starts from a point of lower beam quality $\{2.5\text{kA}, 2\text{mm-mrad}, 6\text{MeV}\}$ and finish at a point of higher beam quality $\{5\text{kA}, 1\text{mm-mrad}, 3\text{MeV}\}$ on a straight line pass in the 3D space. By defining a Beam Quality Factor (BQF), which goes from 0 to 1 linearly as the operation goes from the starting to the finishing points, we may visualize in Fig.3 the effect of such an upgrade pass over a broad wavelength range. Notice the factor of 2 change in each beam quality parameter between the two points.

IV. ACKNOWLEDGMENT

I thank Herman Winick for discussions on LCLS optimization scheme, Schlomo Caspi for providing parameters for the superconducting helical wiggler and Kwang-Je Kim for discussions on SASE physics.

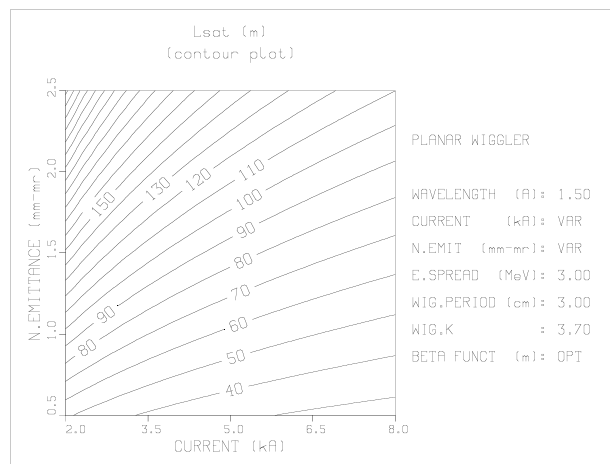


Figure 2. L_{sat} vs. I and ε_n for the hybrid wiggler with $g = 0.6$ cm.

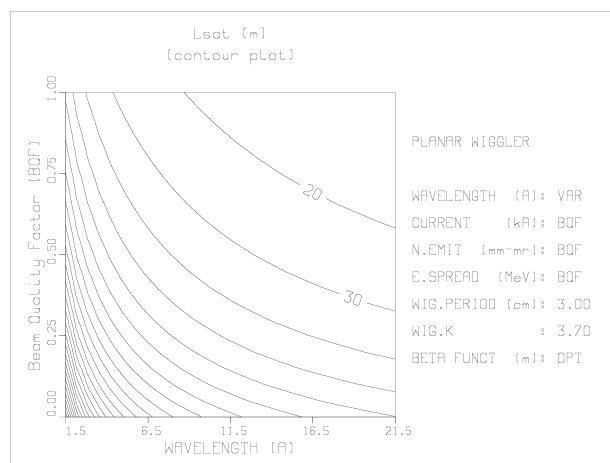


Figure 3. L_{sat} vs. λ and beam quality factor for the hybrid wiggler with $g = 0.6$ cm.

References

- [1] H. Winick et al., NIM. A347 (94) 199.
- [2] K.-J. Kim, NIM. A250 (86) 396. PRL.57 (86) 1871.
- [3] J.-M. Wang, L.-H. Yu, NIM. A250 (86) 484.
- [4] R. Bonifacio et al., PRL. 73 (1994) 70.
- [5] L.-H. Yu, S. Krinsky, NIM. A285 (89) 119.
- [6] L.-H. Yu et al., Phys.Rev. E51 (95) 813.
- [7] G. Travish, J. Rosenzweig, Proc. PAC (93) 1548.
- [8] R. Bonifacio et al., Opt. Comm. 50 (84) 373.
- [9] L.-H. Yu, S. Krinsky, R.L. Gluckstern, PRL. 64 (90) 3011.
- [10] Y.H. Chin, K.-J. Kim, M. Xie, Phys. Rev. A46 (92) 6662.
- [11] M. Xie, to be published.
- [12] K.-J. Kim, M. Xie, NIM. A331 (93) 359.
- [13] W.M. Fawley et al., Proc. PAC (93) 1530.
- [14] K. Halbach, J.Phys. (Paris) Colloq. 44 (83) C1-211.
- [15] S. Caspi, LBL tech-note, SC-MAG-475 (94).